RSC Advances

ROYAL SOCIETY OF CHEMISTRY

www.rsc.org/advances

Journal Name

COMMUNICATION

Preparation of Nanoporous molybdenum film by Dealloying Immiscible Mo-Zn System for hydrogen evolution reaction

Received 00th January 20xx,
Accepted 00th January 20xx

DOI: 10.1039/x0xx00000x

www.rsc.org/

Zixin He, Yuan Huang* and Fang He*

Nanoporous Mo film was prepared by dealloying immiscible Mo-Zn system. The successful dealloying owed to the long-distance diffusion of Mo atoms (~600nm) in nanocrystalline Zn layer during annealing. The obtained NPMF exhibited a good activity toward hydrogen evolution reaction, with a Tafel slope of 85 mv dec^{-1}.

Chemical/electrochemical dealloying, as a well-known process for the selective dissolution of one or more active metal components from alloys, is widely used to generate three-dimensional (3D) porous metals with bicontinuous ligament-pore structure, which have attracted great interest in a lot of technological applications such as catalysis, full cells, surface-enhanced Raman scattering (SERS),[1-3] owing to their high surface area and high strength. To date, numerous nanoporous metals such as np-Au,[4] np-Ag[5] and np-Pt[6] have been prepared through dealloying and all of these materials have some excellent performance in certain applications.

Although dealloying has been extensively studied and many valuable research results have been achieved in this field, more investigations are still needed to be done. For example, many non-precious metals have a lot intriguing physical and chemical properties. Fabricating those nanoporous metals through dealloying would be of great importance in some application fields. Although some non-noble porous metals including Ni, Cu, Ti, Fe, Cr, Bi, Ga, Sn have been fabricated through dealloying,[7-11] it is still meaningful to prepare more new non-noble porous metals. In addition, besides common solid solutions, intermetallic compounds and metallic glasses, more alloy systems which are suitable for dealloying to fabricate nanoporous metal should be developed.

Here we report a new nanoporous metal by dealloying an immiscible alloy system. Unlike ordinary miscible alloy systems, the heat of mixing of immiscible alloy systems is positive($\Delta Hm > 0$),[12] which means that the elements of immiscible alloy systems are, in general, difficult to diffuse even at high temperature, in other words, immiscible alloy systems cannot be utilized to dealloying unless there is a sufficient diffusion among the components of immiscible alloy systems to form new compounds .

To solve the difficulty for the elements diffusion of immiscible alloy system, nanocrystallization of one or both of the immiscible elements seems to be an appropriate way. On the one hand, in contrast to their coarse-grained polycrystalline counterparts, the atomic diffusivities in nanocrystalline materials are often several orders of magnitude larger.[13, 14] For example, Wang and his coworkers[15] prepared a layer of nanocrystalline Fe on the top of an iron plate and they found the diffusion coefficient for Cr in nanocrystalline Fe was 7-9 orders of magnitude larger than that in coarse-grained Fe.

In this work, a novel nanoporous Mo film (NPMF) was successfully formed by dealloying immiscible Mo-Zn system (the Mo-Zn phase diagram is illustrated in Fig. S1). The as-prepared NPMF shows good activity for hydrogen evolution reaction, indicating it a promising non-precious electrocatalyst for hydrogen evolution reaction (HER).

Mo foils (12μm thickness) were cleaned in solution of 0.9M H_2SO_4 and 0.6M HCl for 3 min and then dipped into solution containing 0.8M Cr^{6+} and 2.5M H^+ for 10 min to remove oxide film. Then a Zn layer was cathodic electrodeposited on Mo substrates (9cm^2 exposed area) in the electrolyte solution with 0.4M $ZnCl_2$, 2.7M KCl, 0.4M H_3BO_3 and 20ml L^{-1} Zn-plating softening agent at room temperature. The electrodeposition process was conducted in a two-electrode cell, with Zn plate as counter electrode, the current density was set to 20mA cm^{-2} and the deposition time was controlled to be 5 min. After being rinsed extensively with deionized water and dried in a vacuum chamber, the Mo/Zn bilayered samples were annealed at 400°C for 5h under the protection of Ar gas. Then the selective dissolution of Zn was conducted by immersing the annealed Mo/Zn bilayered samples in concentrated nitric acid. Finally, the as-dealloyed samples were immersed in 2% NaOH aqueous solution for 5 min to remove the oxide film which was generated during dealloying and then rinsed by deionized water and dried in a vacuum chamber again for

Tianjin Key Laboratory of Composite and Functional Materials, School of Material Science and Engineering, Tianjin University, Tianjin 300072, PR China.

E-mail: profhy_tju@sina.cn; tju_hefang@sina.cn

†. Electronic Supplementary Information (ESI) available: Mo-Zn phase diagram, AES depth profiles of bilayered Mo/Zn bilayered sample annealed at 400°C and a high magnification TEM image of electrodeposited Zn layer *after annealing.* See DOI: 10.1039/x0xx00000x

further analysis. After that, the microstructure and chemical analysis of as-obtained NPMF was characterized by scanning electron microscopy (SEM, Hitachi S4800) equipped with an energy-dispersive X-ray spectrometer (EDS). N_2 adsorption/desorption experiment was conducted at 77K using a BK132F surface analyzer to obtain the pore size distribution of the as-obtained NPMF. The phase structure was analyzed by X-ray diffraction (XRD, Rigaku D/max 2500 CuKα). The composition distribution of the annealed Mo/Zn bilayered sample was detected by means of Auger depth profiles (AES, PHI-700, sputtering rate for SiO_2/Si is 25nm/min). The microstructure of Mo-Zn interface was investigated by transmission electron microscopy (TEM, Tecanai G2 F20 S-Twin) operating at 200kv. Line scanning of EDS analysis was performed from the electrodeposited Zn layer to Mo substrate across the Mo/Zn boundary to obtain the composition gradient.

The electrochemical reduction of hydrogen was carried out in a 0.5M H_2SO_4 aqueous solution using an electrochemical workstation (Gamry Interface 1000). A platinum plate and a saturated calomel electrode (SCE) were used as counter electrode and reference electrode, respectively. The NPMF and a cleaned smooth Mo foil were used as working electrodes, respectively. The area of the working electrodes immersed into the electrolyte solution was controlled to be ~1cm^2.

The microstructure of NPMF is illustrated in Fig.1 (a-c). Crack-free NPMF with an average pore size of ~200nm (Fig.1a) and a film thickness of ~300nm (Fig.1b) was fabricated by immersing 400°C annealed Mo/Zn bilayered sample in concentrated HNO_3 for 4h at room temperature. The composition of nanoporous film was characterized by EDX analysis and only ~2.68 at.% Zn still remained (Fig.1c). The residual Zn was probably existed in the surface region of Mo substrate which was passivate during dealloying. Fig.1d presents nitrogen adsorption/desorption isotherm obtained on the as-dealloyed sample. Obviously, the absorption isotherm is classified as type III. Pore size distribution of NPMF (inset of Fig.1d) was estimated by the Barrett-Joyner-Halenda (BJH) method.[16] One can see that the main pore radius is over 100nm and the max pore radius is ~ 240 nm which is consistent with SEM observation.

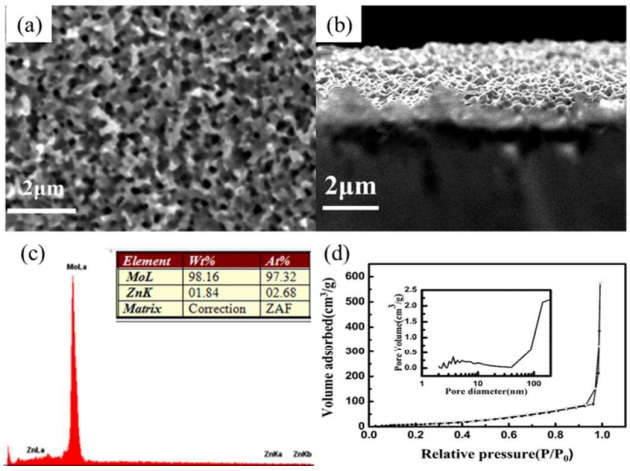

Fig.1 (a) plane view and (b) section view SEM images of Mo-Zn bilayered samples annealed at 400°C for 5h and then dealloyed in concentrated nitric acid for 4h; (c) EDS spectrum of the dealloyed Mo-Zn sample, (d) N_2 adsorption-desorption isotherm for the dealloyed Mo-Zn sample; adsorption-solid symbol, desorption-hollow symbol, the inset shows the pore size distribution of the obtained NPMF.

Now, the intrinsic reason why the annealed Mo/Zn bilayered sample can be successfully dealloyed is discussed. The XRD patterns of Mo/Zn bilayered samples before and after annealing as well as the as-dealloyed sample are shown in Fig.2a, from which it can be seen the patterns of the samples before and after annealing are all consisted of metallic Mo and Zn. Besides, it is clear that only a body centered cubic (b.c.c) Mo phase can be identified in the dealloyed sample. Considering the strong signal of Mo substrate may cover some extra information, GIXRD, a unique technology to evaluate the phase structure of thin film was used to analyse the phase structure of Mo/Zn bilayered samples. Fig.2b shows the GIXRD patterns of Mo/Zn bilayerd samples before and after annealing as well as the dealloyed sample. It can be seen that the sample before annealing is just consist of metallic Zn and Mo and the dealloyed sample only contains Mo phase, while some light diffraction peaks of $MoZn_{22}$ intermetallic phase are observed for the sample annealed at 400°C. All the above results indicate that the content of $MoZn_{22}$ is very low, thus, the $MoZn_{22}$ has very limited contribution to the dealloying and the formation of NPMF. Besides, there is one more evidence supporting that $MoZn_{22}$ has little influence on the dealloying process to fabricate NPMF, i.e. the content of noble element (Mo) of this phase is only ~ 4.4at%, indicating that the material which was even composed of homogeneous $MoZn_{22}$ cannot be used to prepare bicontinuous nanoporous structure through dealloying.[17] Thus, we consider that there should be another key issue for the successful dealloying of immiscible Mo-Zn system.

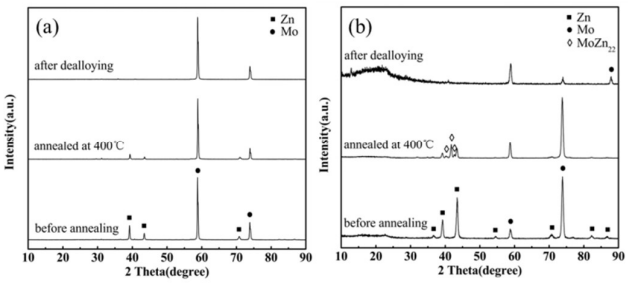

Fig.2 (a) XRD and (b) GIXRD patterns of Mo-Zn bilayered samples as well as the dealloyed samples. The incident angle in the GIXRD experiment was 2°.

The typical Auger depth profiles of Mo, Zn elements in the annealed Mo-Zn bilayered samples are illustrated in Fig. S2, which confirm that the obvious diffusion occurred between the immiscible Mo and Zn elements in the Mo-Zn bilayered sample after annealing at 400°C for 5h. Since the details of the diffusion are still unclear, thus, the microstructure of Mo-Zn interface was further investigated by TEM, and the results was shown in Fig.3. Fig.3a displays a cross-sectional TEM view of the interface of annealed Mo/Zn bilayered sample, Fig.3b shows the selected area electron diffraction (SAED) pattern of the region marked with "A" in Fig.3a,

verifying that the region A is composed of Mo, and Fig.3c displays the SAED patterns of the region marked with "B" in Fig.3a, verifying that the region B is composed of hcp-structured Zn. Fig.3d shows the composition profiles obtained by performing a line-scanning along the white arrow marked in Fig.3a. It can be seen that Mo atoms diffused a long distance (~600nm) in Zn layer which is much deeper than the results obtained in other similar work, such as Cu/Fe (25nm),[18] Cu/Ta (10nm)[19] and even swift heavy ion irradiated UMo/Mg (110nm).[20]

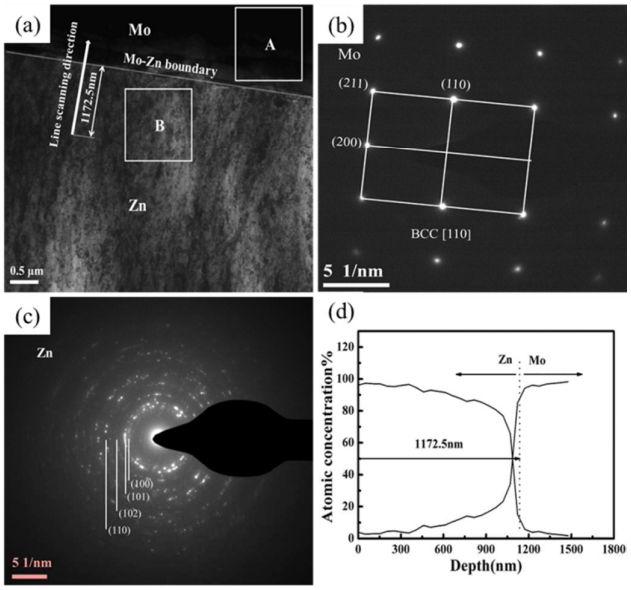

Fig.3 (a) cross-sectional TEM observation of the interface of Mo substrate and electrodeposited Zn layer; (b) and (c) shows the SAED patterns of Mo substrate and Zn layer, the diffraction area correspond to the square a and b in Fig.3(a), respectively; (d) line scanning curves along the white arrow in Fig.(a), the dash line corresponds to the Mo-Zn boundary in Fig.3(a).

We speculate the long-distance diffusion of Mo atoms in Zn layer could be attributed to the nanocrystalline structure of Zn layer. Firstly, the average grain size of Zn layer after annealing is calculated to be 32.6nm by using Scherrer analysis according to the peak width of (100), (101) and (110) of the diffraction pattern shown in Fig.2a, which is comparable with those observed from the high magnification TEM view of Zn layer (15-50nm) shown in Fig. S3, indicating there are a great deal of grain boundaries in nanocrystalline Zn layer. These defective grain boundaries can provide "short-circuit" channels for atomic diffusion.[21] Secondly, when the Mo/Zn bilayered sample was annealed at 400°C, some small Zn grains was in semi-solid state due to the size-dependent melting point phenomenon,[22] then some atoms in instability area would get enough energy and break away from the original equilibrium position, leading to the formation of vacancies.[23] Simultaneously, the atomic thermal migration in normal crystal lattice near the melting point would also cause the formation of vacancies.[24] All these vacancies would promote the diffusion of Mo atoms in Zn layer.

It is obvious that the diffusion depth of Mo atoms should be longer than the thickness (~300nm) of the obtained NPMF (Fig. 1b), The long-distance diffusion of Mo atoms in Zn layer is propitious to the agglomeration and integration of Mo atoms during dealloying, which is good for the formation of the nanoporous layer on the substrate. According to the above discussions, we consider the intrinsic reason of successful dealloying of annealed Mo/Zn bilayered sample could be attributed to the long-distance diffusion of Mo atoms in Zn layer.

Fig.4a presents the linear scan voltammograms polarization curves for as-obtained NPMF, smooth Mo foil and bare platinum electrode. It can be seen that NPMF exhibits better HER activity than smooth Mo since NPMF have much more specific surface area than smooth Mo. Tafel plots of these catalysts were recorded with the linear regions fitted into Tafel equation (η= blog j+a, where j is the current density and b is the Tafel slope). A smaller Tafel slope means a faster increase of HER rate with the increase of applied potentials. The Tafel slopes for smooth Mo, NPMF and bare platinum electrode are 164, 85 and 62 mv dec^{-1} (Fig. 4b), respectively. Obviously, NPMF presents a much faster electron transfer rate than smooth Mo due to its lower Tafel slope which is close to those of CoP (76mv/dec),[25] Ni_2P (70mv/dec)[26] and WC (84mv/dec),[27] indicating NPMF is a promising electrocatalyst for HER. Furthermore, the obtained NPMF could serve as a nanoporous skeleton for decorating other nanoparticles which are efficient in HER, due to its relative large pore/ligament size.

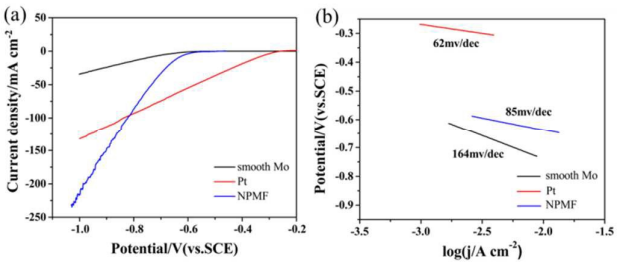

Fig.4 (a) LSV polarization curves for NPMF, smooth Mo and bare platinum plate, the scan rate is 2mv/s; (b) Tafel plots of NPMF, smooth Mo and bare platinum plate.

In summary, a new dealloying approach based on an immiscible alloy system is presented in this paper. Nanoporous Mo film was prepared on Mo substrate by a three step process involving electrodeposition of a layer of nanocrystalline Zn on molybdenum substrate, annealing at high temperature and finally etching of Zn atoms. The nanocrystallization of zinc grains is necessary for the adequate diffusion of Mo atoms in Zn layer and the following dealloying process. The obtained NPMF possesses superior catalytic performance than smooth Mo foil in hydrogen evolution reaction, indicating it a promising non-precious electro-catalyst for HER.

Acknowledgements

The authors would like to acknowledge the National Natural Science Foundation of China (Grant No. 51171128; 51471114), and the Key Technologies R & D Program of Tianjin (Grant No. 11ZCKFGX03800) for providing financial support for this research.

Notes and references

1 Z. H. Zhang, C. Zhang, J. Z. Sun, T. Y. Kou and C. C. Zhao, *RSC Adv,*, 2012, **2**, 11820-11828.
2 H.-J. Qiu, Y. Ito and M. W. Chen, *Scri. Mater*., 2014, **89**, 69.
3 H. Y. Fu, X. Y. Lang, C. Hou, Z. Wen, Y. F. Zhu, M. Zhao, J. C. Li, W. T. Zheng, Y. B. Liu and Q. Jiang, *J. Mater. Chem. C*., 2014, **2**, 7216.
4 Z. H. Zhang, C. Zhang, Y. L. Gao, J. Frenzel, J. Z. Sun and G. Eggeler, *CrystEngComm*, 2012, **14**, 8292-8300.
5 T. T. Song, T. L. Gao, Z. H. Zhang and Q. Z. Zhai, *CrystEngComm*, 2011, **13**, 7058.
6 S. H. Kim, J. B. Choi, Q. N. Nguyen, J. M. Lee, S. Park, T. D. Chung and J. Y. Byun, *Phys. Chem. Chem. Phys.,* 2013, **15**, 5782.
7 J. Cai, J. Xu, J. M. Wang, L. Y. Zhang, H. Zhou, Y. Zhong, D. Chen, H. Q. Fan, H. B. Shao, J. Q. Zhang and C. N. Cao, *Int. J. Hydrogen Energy*., 2013, **38**, 934-941.
8 F. L. Jia, J. H. Zhao and X. X. Yu, *J. Power Sources*., 2013, **222**, 135-139.
9 T. Wada, K. Yubuta, A. Inoue and H. Kato, *Mater. Lett*., 2011, **65**, 1076-1078.
10 T. Wada and H. Kato, *Scri. Mater*., 2013, **68**, 723-726.
11 Z. H. Zhang, Y. Z. Wang and Y. Wang, *J. Nanosci. Nanotechno*., 2013, **13**, 1503-1506.
12 E. Ma, *Prog. Mater. Sci*., 2005, **50**, 413.
13 H. Gleiter, *Prog. Mater. Sci.*, 1989, **33**, 223.
14 Y. R. Kolobov, G. P. Grabovetskaya, M. B. Ivanov, A. P. Zhilyaev and R. Z. Valiev, *Scri. Mater*., 2001, 44, 873.
15 Z. B. Wang, N. R. Tao, W. P. Tong, J. Lu, K. Lu, *Acta Mater*., 2003,**51**, 4319.
16 E. P. Barrett, L. G. Joyner, P. P. Halenda, *J. Am. Chem. Soc*., 1951, **73**, 373.
17 H.-J. Qiu, L. Peng, X. Li, H.T. Xu, Y. Wang, *Corros. Sci*., 2015, **92**, 16.
18 Y. H. Yang, D. Z. Wang, J. Lin, D. F. Khan, G. Y. Lin and J. D. Ma, *Mater. Des*., 2015, **85**, 635.
19 H. J. Lee, K. W. Kwon, C. Ryu and R. Sinclair, *Acta Mater*., 1999, 47, 3965.
20 H.-Y. Chiang, M. Doblinger, S.-H. Park, L. Beck and W. Petry, *J. Nucl. Mater*., 2014, **453**, 41.
21 X. Sauvage, G. Wilde, S. V. Divinski, Z. Horita and R. Z. Valiev, *Mater. Sci. Eng: A*., 2012, **540**, 1.
22 K. K. Nanda, S. N. Sahu and S. N. Behera, *Phys. Rev. A*., 2002, **66**, 013208.
23 G. B. Er, P. J. Li and L. J. He, Scientia. *Sinica. Phys, Mech & Astron*., 2010, **40**, 1071.
24 M. J. Pozo, S. Davis and J. Peralta, *Physica B*., 2015, **457**, 310.
25 Q. Liu, J. Tian, W. Cui, P. Jiang, N. Chen, A. M. Asiri and X. Sun, *Angew. Chem*., 2014, **126**, 6828.
26 X. B. Chen, D. Z. Wang, Z. P. Wang, P. Zhou, Z. H. Wu and F. Jiang, *Chem. Comm*., 2014, **50**, 11683.
27 A. T. Garcia-Esparza, D. Cha, Y. Ou, J. Kubota, K. Domen and K. Takanabe, *ChemSusChem*., 2013, **6**, 168-181.

Graphical and textual abstract

Nanoporous Mo film was prepared by dealloying immiscible Mo-Zn system and it shows superior catalytic activity towards hydrogen evolution reaction than smooth Mo foil.